Linear and Nonlinear Response of a Rectangular Plate Measured with Continuous-Scan Laser Doppler Vibrometry and 3D-Digital Image Correlation

David A. Ehrhardt
Graduate Research Assistant
Department of Engineering Physics, University of Wisconsin-Madison,
1500 Engineering Drive, Madison, WI 53706

Shifei Yang
Development Specialist
Praxair Inc. 175 East Park Drive Tonawanda, NY 14150

Timothy J. Beberniss
Aerospace Structures Engineer
Structural Sciences Centers, Aerospace Systems Directorate, Air Force Research Laboratory,
Wright-Patterson AFB, OH 45433

Matthew S. Allen
Associate Professor
Department of Engineering Physics, University of Wisconsin-Madison,
1500 Engineering Drive, Madison, WI 53706

Abstract

Dynamic measurement of real structures, such as panels, can be difficult due to their low mass and complicated deformations under large amplitude loading conditions. These conditions bring to light shortcomings of traditional sensors such as accelerometers, strain gauges, displacement transducers, etc. A majority of these sensors require contact with the structure under test which tends to modify the dynamic response of these light structures. In contrast, a few recently developed techniques are capable of measuring the response over a wide measurement field without contacting the structure, which is ideal for these structures. Two techniques are considered here: continuous-scan laser Doppler vibrometry (CSLDV) and high speed three dimensional digital image correlation (3D-DIC). Both techniques can be used to return real-time deformation shapes under certain conditions; however, measurements will be obtained using post processing here. The linear and nonlinear deformations of a clamped flat plate under steady state sinusoidal loading will be measured using both techniques and compared with a finite element model to assess the relative merits of each measurement approach.

Keywords: Continuous Scan, Laser Doppler Vibrometer, Digital Image Correlation, Nonlinear Deflection

1 Introduction

With the development of high performance light weight structures there is an increasing need for experimental techniques capable of measuring the response at a large number of measurement degrees of freedom without modifying the structural response significantly. Techniques such as Continuous-Scan Laser Doppler Vibrometry (CSLDV) and high-speed Three Dimensional Digital Image Correlation (high-speed 3D-DIC) have been developed to meet this need. Both CSLDV and high-speed 3D-DIC are non-contact, non-destructive, and capable of measuring the response at thousands of points across the surface of the test specimen. However,

these techniques involve additional processing to extract velocities or displacements from measured signals when compared with traditional measurement techniques. Both techniques are capable of providing "real-time" measurements; however this has seen limited to no implementation. In the case of 3D-DIC, the computations and amount of data to be handled are significant enough to make this challenging, and limits its application to sampling frequencies of 100Hz. In principle CSLDV could be performed in real time with the implementation of the harmonic power spectrum, but this has not been done yet. For this work, the data acquired with both methods was analyzed in a post-processing step.

CSLDV is an extension of traditional Laser Doppler Vibrometer (LDV) measurements, where the laser point, instead of dwelling at a fixed location, is continuously moving across a measurement surface. This added motion requires the measurement to be treated as time-varying, but the motion also provides an increased measurement resolution with a drastically decreased measurement time when compared with traditional LDV measurements. Several algorithms have been devised to process CSLDV measurements so the vibration shapes of a test piece along the laser scan path can be determined. For example, Ewins et al. treated the operational deflection shape as a polynomial function of the moving laser position [1-5]. They showed that harmonics appear in the measured spectrum separated by the scan frequency, and the amplitudes of these harmonics can be used to determine a polynomial's coefficients that describe the operating deflection shape along the scan path. Allen et al. later presented a lifting approach for impulse response measurements [6, 7]. This approach groups responses at the same location along the laser path so the responses appear to be from a set of pseudo sensors attached to the structure. Conventional modal analysis routines can then be used to determine modal properties of the structure. Recently, algorithms based on Linear Time Periodic (LTP) system theory [8-12] were used to derive input-output transfer functions from CSLDV measurements allowing virtually any input to be used with CSLDV. The algorithms based on LTP system theory will be used in this investigation to identify the natural frequencies and modes shapes of a clamped rectangular plate.

Displacements measured with 3D-DIC are obtained by matching a measurement point, consisting of a pixel area, in each image between each camera for the duration of the experiment. For sample rates greater than 100 fps, deformations are measured using post processing. Schmidt et al. [13] presented early work on the use of high-speed digital cameras to measure the deformation and strain experienced by test articles under impact loadings. Tiwari et al. [14] used

two high-speed CMOS cameras in a stereo-vision setup to measure the out of plane displacement of a plate subjected to a pulse input. Results compared favorably with work previously published and showed the capability of the 3D-DIC system in a high-speed application, although over a short time history. Niezrecki et al. [15], Helfrick et al. [16], and Warren et al. [17] obtained linear mode shapes using 3D-DIC with different test articles using discrete measuring points. Niezrecki et al. and Helfrick et al. also combined accelerometers, vibrometers, and dynamic photogrammetry to compare results obtained with DIC analyzed at discrete measurement locations. Each technique provided complimentary results between all single point measurement techniques showing the capability of 3D-DIC. Since 3D-DIC has the capacity to measure thousands of 3D displacements on a surface, a further comparison can be made with full field measurements if sensor arrays are available; however, handling the large amount of data in conjunction with the image files and measurement locations can prove to be difficult.

These methods are also desired as a tool for nonlinear model updating, where a geometrically nonlinear finite element model (FEM) of the structure is updated to reflect the nonlinear response of the test article [18, 19]. For example, in [19] Allen and Weekes found that the nonlinear response of a finite element model exhibited coupling between two of the linear modes and that the degree of coupling influenced how the resonance frequency changed with amplitude. However, measurements were only available at one point so the FEM could not be confidently updated to reflect the behavior of the test article.

This work seeks to expand on a previous comparison [20] between CSLDV and high-speed 3D-DIC by examining the suitability of these measurements in the linear and nonlinear dynamic response regimes of a 177mm x 228mm clamped aluminum plate. The linear response of the plate was measured when it was excited with a sinusoid at the first and fourth natural frequency. The nonlinear response of the plate was measured when it was excited at high amplitude near the first resonance. CSLDV measurements were processed with the harmonic transfer function and used to identify the mode shapes and natural frequencies. 3D-DIC measurements were processed using a commercial software Aramis [21] and its Real Time Sensor extension [22]. Then a transfer function is assembled and used to identify the mode shapes and natural frequencies of the structure. The quality of the measurements was compared as well as practical considerations that may limit the applicability of the methods.

2 Measurements

2.1 Introduction to CSLDV

CSLDV measurements are acquired by moving the point of a laser-doppler vibrometer (LDV) across a surface using a two dimensional pattern. Patterns can range from simple lines and circles to complex Lissajous curves, but, if the pattern is periodic, the same technique can be used to extract velocities along the pattern no matter what the shape. Note that this work considers only periodic scan patterns, but if the methods developed by Ewins are used then the laser may scan non-periodically over the surface extracting the deformation over a very dense grid [1-5]. In this work, a pattern is scanned across a surface using a single point fiber optic LDV and external mirrors offset from the measurement surface as shown in Figure 1. Retro-reflective tape cut in the shape of the scanning pattern is also added to reduce signal contamination from the speckle pattern needed for 3D-DIC and improve measurement feedback. With the completion of the scan, the LDV measurement is now a collection of time-varying velocities of the surface deformation in the defined z-direction. The measured data are analyzed using the harmonic transfer function concept from linear-time periodic (LTP) systems, which is derived by defining an exponentially modulated periodic signal, and using the general solution for the response of a linear time varying system [23]. This allows the user to employ LTP algorithms that are analogous to the transfer function of linear time invariant (LTI) systems, and can be written in a modal summation form in terms of the modal parameters of the structure. For further discussion, the reader is referred to [11, 24, 25].

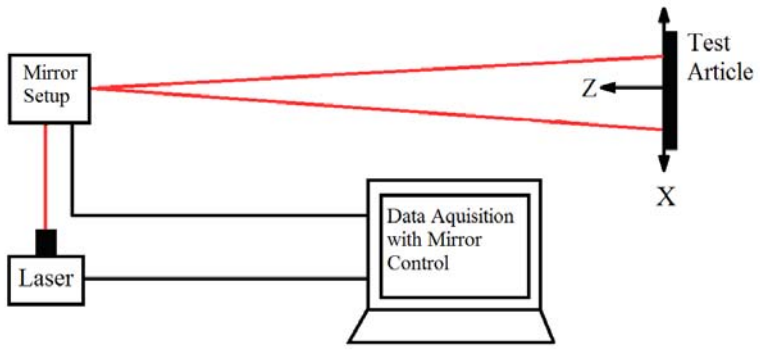

Figure 1: CSLDV System Diagram: The laser beam was redirect by a pair of mirrors to continuously scan on the test article

This method of mode shape extraction has previously been successfully applied to 1-D single frequency line scans on beams [20, 25], and is readily applied to CSLDV measurements

with a more complicated scanning pattern, provided the scan pattern is periodic. Here, a Lissajous curve is used, which defines the x- and y-coordinate of the pattern as a system of parametric equations shown in Equation (1. The x- and y-coordinates oscillate at separate frequencies, f_x and f_y, and are defined as 90 degrees out of phase. The result is a closed periodic scan pattern allowing the use of the previously mentioned LTP algorithms. The period of the Lissajous curve can then be defined as the smallest period within which both f_x and f_y have an integer number of cycles as shown in Equation (2, where T_x and T_y are the periods of the x- and y- positions of the laser. Using this definition, N_x and N_y are defined based on the ratio of the selected x- and y-coordinate frequencies, as shown in Equation (3(3(3(3. The selection of scan frequencies involves considerations of the measurement area to be covered, the measurement noise (which generally increases with the speed of the moving laser), the expected spatial density of the deformation, and level of damping and modal density of the structure. The level of damping and modal density is especially important when using broad band methods of excitation [25], which is not used here. In this work, the x-coordinate frequency is set as 3Hz and the y-coordinate frequency is set as 4Hz to keep feedback noise from the laser low while providing enough measurement signal to distinguish complex deformation shapes. The result is a Lissajous curve, shown in Figure 3a, with a period of 1Hz.

$$\begin{aligned} x(t) &= A_x \cos(2\pi * f_x t) \\ y(t) &= A_y \sin(2\pi * f_y t) \end{aligned} \tag{1}$$

$$T_{Lissajous} = N_x * T_x = N_y * T_y = N_x * \left(\frac{1}{f_x}\right) = N_y * \left(\frac{1}{f_y}\right) \tag{2}$$

$$\frac{N_x}{N_y} = \frac{f_x}{f_y} \tag{3}$$

2.2 Introduction to 3D-DIC

For digital image correlation, two cameras are used to image the test article as it deforms and then the 3D displacements of the surface can be determined using digital image correlation (DIC) algorithms, which match portions of the surface from image to image and use that to

calculate the displacements. As schematically shown in Figure 2, the two cameras are placed at a specific distance along the Z-axis from the test article to allow the surface to be captured simultaneously in each camera and establish a field of view. A pan angle, Θ_p, is specified based on a desired depth of view or the range of out-of-plane displacements expected. Once the stereo camera setup is assembled and fixed, photogrammetric principles of triangulation and bundle adjustment are used to establish each camera's position and the experimental measurement volume by capturing images of a known pattern or calibration panel [26]. With this calibration, displacement accuracy is not limited to the pixel size of the imaged surface, but allows for accuracies on the sub pixel level (eg. 0.1 pixels). Prior to testing, a high-contrast random speckle pattern is applied to the measurement surface to increase image texture and improve image correlation.

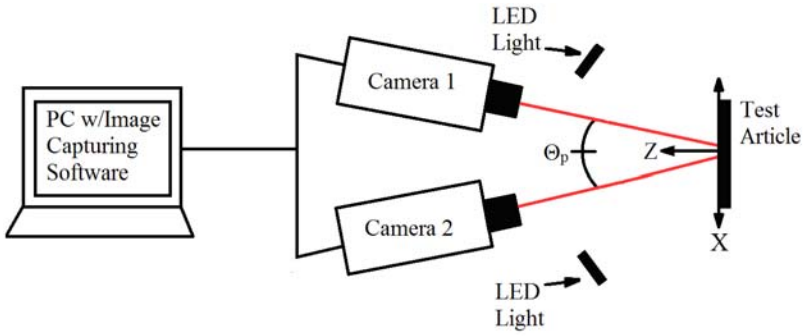

Figure 2: 3D-DIC System Diagram**.** The 3D-DIC system diagram shows Camera 1 (left camera) and Camera 2 (right camera) set to a specified pan angle, Θ_p.

In this work, a commercial software (Aramis [21]) is used to calibrate and analyze displacements of the measurement surface. The high-contrast random speckle pattern is applied to the surface using the best practice discussed in [27] based on the desired field of view. The use of retro-reflective tape for CSLDV measurements results in contamination of 3D-DIC measurements where the tape covers the speckle pattern as seen in the static 3D-DIC measurements in Figure 3b. So, results for dynamic 3D-DIC presented in this paper will be from a selection of measurement points around this Lissajous scan pattern.

3 Test and Analysis Description

3.1 Test Specimen and Finite Element Model

The device under test for this investigation is a nominally flat clamped aluminum plate. As summarized in Table 1, the tested plate had an effective length of 177mm, an effective width

of 228mm, and a thickness of 0.5mm. The plate was then clamped between two mounting frames with adhesive as further described in [28]. After being fixed between the mounting frames, the plate was painted with a white base coat, and a speckle pattern was applied using a marker and spray paint to increase the imaged surface texture and improve tracking for both 3D-DIC systems. Once the plate had dried, a pattern of retro-reflective tape cut from a printed Lissajous stencil was added to increase feedback to the CSLDV laser while providing room for 3D-DIC measurements. The final prepared plate is shown in the clamping fixture in Figure 3a. For an accurate description of the initial conditions of the plate, static 3D-DIC images were captured after the plate was fully clamped. An initial deflection of 0.613 mm near the center of the plate was measured, as shown in Figure 3b, where the color bar segments the defined z-coordinate. This coordinate system was defined based on the front of the clamping fixture, or 25.4mm from the clamped edge of the plate. One can see that the retro-reflective tape and the edge of the mounting frame have a negative effect on the ability of 3D-DIC to track surface deformations at certain positions, but the measurement density is high in other regions so it is not difficult to interpolate over the anomalies that these introduce. The final step of preparation was the addition of a 6mm steel disk to the back of the aluminum plate to give allow input force from a magnetic driver, discussed in the next section. The location of this disk is shown in Figure 3a.

To provide a baseline of comparison between measurement techniques for linear responses, the finite element model (FEM) described in [28] is used. A coordinate transformation established in the static 3D-DIC measurements is used to match the coordinate system in the FEM with the measurement coordinate systems for CSLDV and 3D-DIC. Low amplitude tests were performed and used to identify the linear natural frequencies and modes shapes for the first and fourth modes, and to compare the results of the two methods. For high amplitude testing, only a comparison between the measured responses is made since geometrically nonlinear simulations with the FEM exceeds time constraints for submission of this paper.

Table 1: Plate Geometric and Material Properties

Length = 177 mm	Width = 228 mm	Thickness = 0.5 mm
E = 71.7 GPa	$\upsilon = 0.33$	$\rho = 2.76*10^3$ kg/m^3

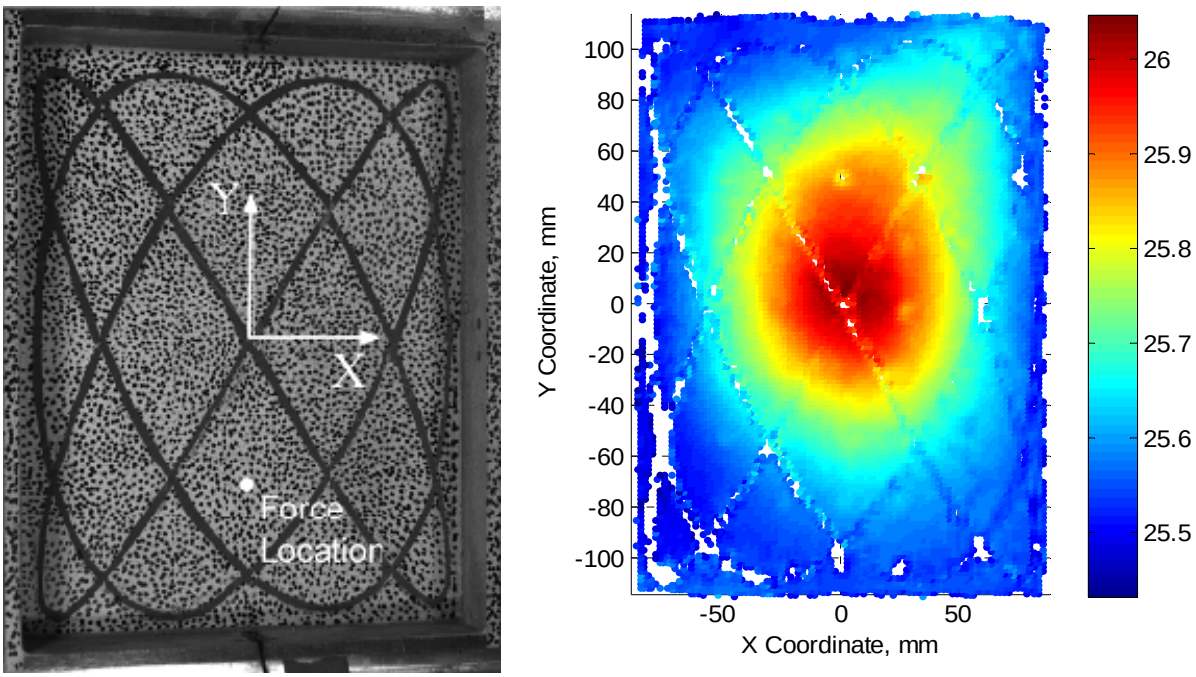

(a) (b)

Figure 3: Images of Rectangular Plate: a) Final prepared surface, b) Measured initial curvature

3.2 Experimental Setup and Description

The experimental setup is shown in **Error! Reference source not found.**. In this setup, there are five main systems: 1) exciter/controller, 2) static 3D-DIC system, 3) dynamic 3D-DIC system, 4) the CSLDV system, and 5) system for force appropriation:

1) Excitation was provided by two separate mechanisms, both controlled in an open-loop using a Wavetek Variable Phase Synthesizer. The low amplitude excitation was provided by a magnetic driver with a Piezo Amplifier. The force exerted by the magnetic driver was measured using a force transducer mounted to a solid base between the magnetic driver providing measurement of the reaction force with the base. Since the plate is aluminum, a small steel disk was added to the plate in the previously described location. High amplitude excitation was provided by shaking the frame on which the plate was mounted with a 5000N MB dynamics shaker and power amplifier. Excitation for this setup is provided through the mounting base at a set excitation acceleration. This type of excitation limits the ability to examine asymmetric modes and why the measurements focused on the first and fourth modes of the plate.

2) The static 3D-DIC system consists of two Prosilica GT2750 CCD cameras with a full resolution of 2750 x 2200 pixels with a maximum frame rate of 20 fps. For this experimental

setup, full resolution images were selected for finer measurement resolution. The static system uses 18mm lenses and is positioned at a standoff distance of 580mm with a camera angle of 26 degrees. All static displacements were determined using a commercial 3D-DIC software Aramis [17] using subsets of 31x31 pixels with a 13 pixel overlap across the entire surface of the plate. A 250mm x 200mm calibration panel was used to establish the measurement volume and lead to a calibration deviation of 0.032 pixels or 0.004 mm for this field of view.

3) The dynamic 3D-DIC system includes two Photron, high speed 12-bit CMOS cameras (model Fastcam SA5 775K-M3K). Each camera has 32GB of memory onboard with a maximum resolution of 1024×1024 pixels. For this experimental setup, images of 704×768 pixels were used to fit as much of the plate in the frame of both cameras as possible. The dynamic system uses 85mm lenses at a stand off distance of 1370mm with a camera angle of 24.4 degrees. All dynamic displacements were determined using a software extension of Aramis called IVIEW Real Time Sensor [18] using subsets of 15x15 pixels. In order to minimize the heat generated and remove the 60 Hz noise produced by the halogen lamps that are typically used in high-speed DIC systems, two 305×305 LED light panels were used. The cameras and the data acquisition system were simultaneously started using an external TTL trigger. Measurement points were selected to avoid the retro-reflective tape, so there is no overlap of measurements between CSLDV and 3D-DIC. This was done to reduce the measurement noise previously seen in the static measurements and provide better tracking for the DIC algorithm. A 250mm x 200mm calibration panel was used to establish the measurement volume and lead to a calibration deviation of 0.02 pixels or 0.007 mm for this field of view.

4) The continuous-scan mechanism was built using a Polytec OFV-552 fiber optic laser vibrometer with a sensitivity of 125 mm/s/V and the same external mirror system that was used in [24, 29]. The mirrors were positioned at a stand off distance of 2.4m, which was selected to minimize the scan angle (5.4 degrees in y-direction) and maintain the specified standoff distance. The external mirror system consisted of two galvanometer scanners in open-loop control; each scanner had a position detector that measured the instantaneous rotational angle, allowing precise and accurate control and measurement of the laser position. The control and data acquisition system was built using a National Instruments PXI system. A LabVIEW program was developed to integrate several the features including the function generator, data acquisition, and signal processing. As previously mentioned, the Lissajous pattern used for this investigation has a x-

direction scan frequency of 3 Hz and a y-direction scan frequency of 4 Hz with a maximum amplitude of 162mm in the x-direction and 211mm in the y-direction. The starting point for the laser, based on the coordinate system set in Figure 3, was at x = 162mm and y = 0. Data was collected at a sampling frequency of 10,240Hz for 2 minutes.

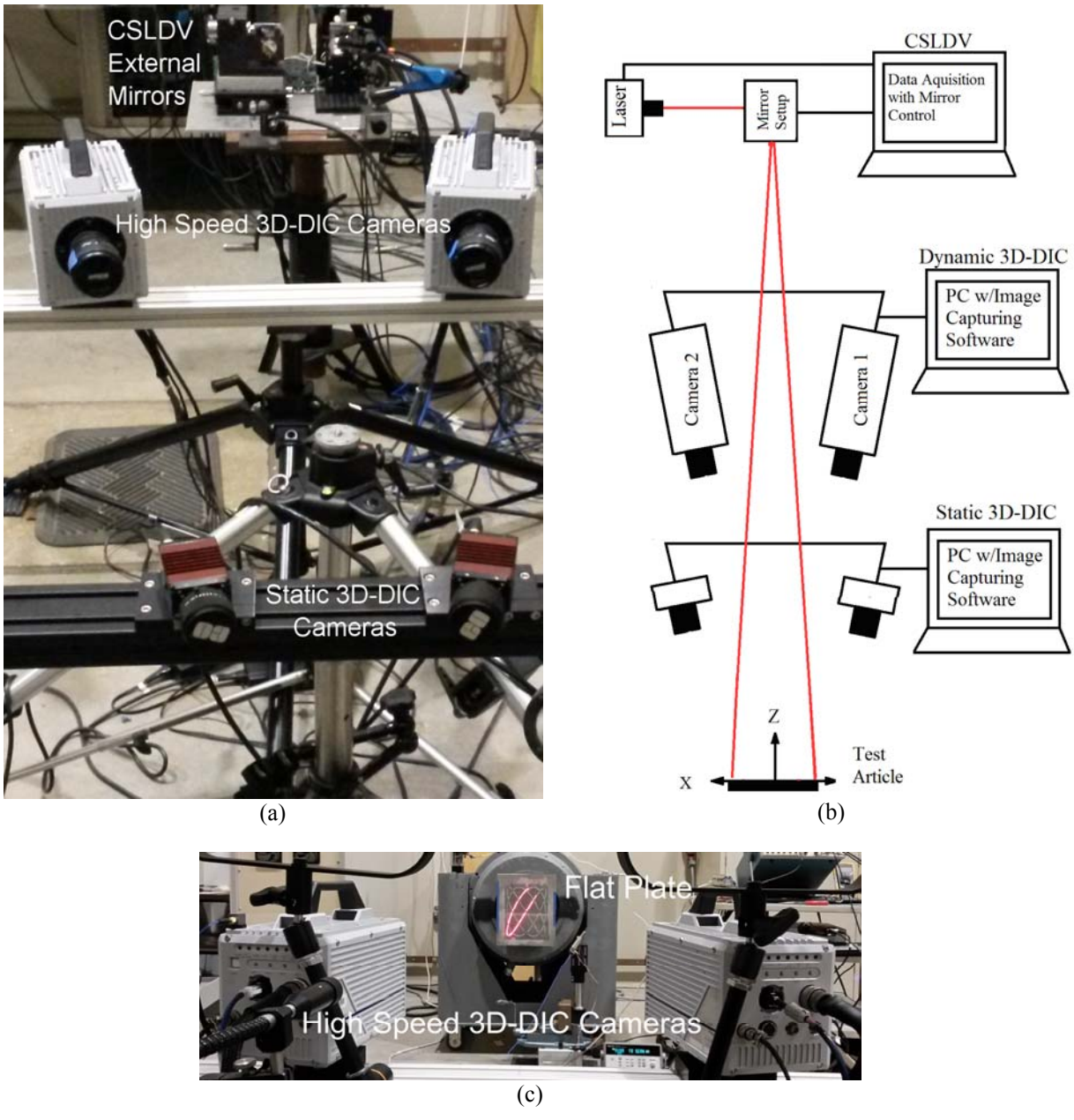

Figure 4: Experimental Setup. a) Measurement Systems, b) Complete experimental schematic, c) Close-up of Rectangular plate

5) A second single point laser is used to measure the response of the plate as it is subjected to a single frequency sinusoid at a set excitation amplitude. Additionally, the voltage

input to the exciter was measured, as well as the input force for the magnetic driver and the base acceleration for the shaker. The velocity response and input voltage signals were analyzed in real time using a Onosoki FFT Analyzer to track the phase between the signals. Here, the input voltage was used instead of the measured force/acceleration to limit noise contamination from the measurement sensors. However, the measured force/acceleration signals were compared after measurement to ensure the correct phase relationship between input and response was maintained. Natural frequencies could then be determined by adjusting the frequency until the input voltage and response velocity are 180 degrees out of phase.

4 Results

4.1 Modal Hammer Test

Single input and single output modal hammer tests were performed on the plate pre- and post-test for each level of excitation to check consistency of the plate's boundary conditions and detect damage throughout testing. Analyzing the frequency response functions (FRFs) obtained from hammer tests revealed that each method of excitation affected the dynamic response of the plate differently. For instance, a consistent reduction of 1Hz in the first natural frequency, was observed with the placement of the magnetic driver in range of the excitation location. Also, 140 Hz noise from shaker cooling fan was measured when the shaker was turned on. Even with these effects a maximum frequency shift of 1.8% was observed in the first natural frequency of the plate, the natural frequency that showed the highest percent change, showing the plate did not change significantly with time. The natural frequencies (f_n) and damping ratios (ζ) from the measured FRFs from each hammer test were averaged and are presented in Table 2. Additionally, the natural frequencies from the FEM are included, which show good agreement with the test frequencies as seen with the calculated percent errors. Although, the added mass from the paint and retro-reflective tape were not included, which could account for the consistently lower values of the natural frequencies.

Table 2: Modal Comparison

Mode		1	2	3	4	5	6	7	8	9
Test	f_n, Hz	106.1	159.4	236.9	276.6	307.8	420.5	436.4	458.9	532.9
	ζ, -	0.79%	1.27%	0.66%	0.66%	0.41%	0.65%	0.41%	0.68%	0.59%
FEM		113.74	195.90	263.75	330.07	339.53	466.90	492.35	512.83	565.4
% Error		-6.72%	-18.63%	-10.18%	-16.20%	-9.35%	-9.94%	-11.36%	-10.52%	-5.75%

4.2 Linear Mode Shape

Force appropriation was used to drive the plate at the first and fourth natural frequency and the steady state response was measured using both CSLDV and high-speed 3D-DIC. Figure 5 shows an example of the spectrum from the CSLDV signal with the Lissajous frequency of 1Hz when the plate was driven at 106.9Hz and 277.7Hz. For mode 1 and mode 4, the sideband harmonics higher than the 14th and 32nd order, respectively, are in the noise of the signal, as seen in the power spectral density (PSD) plots in Figure 5a and 5b, and hence no harmonics above these orders were used when constructing the mode shapes.

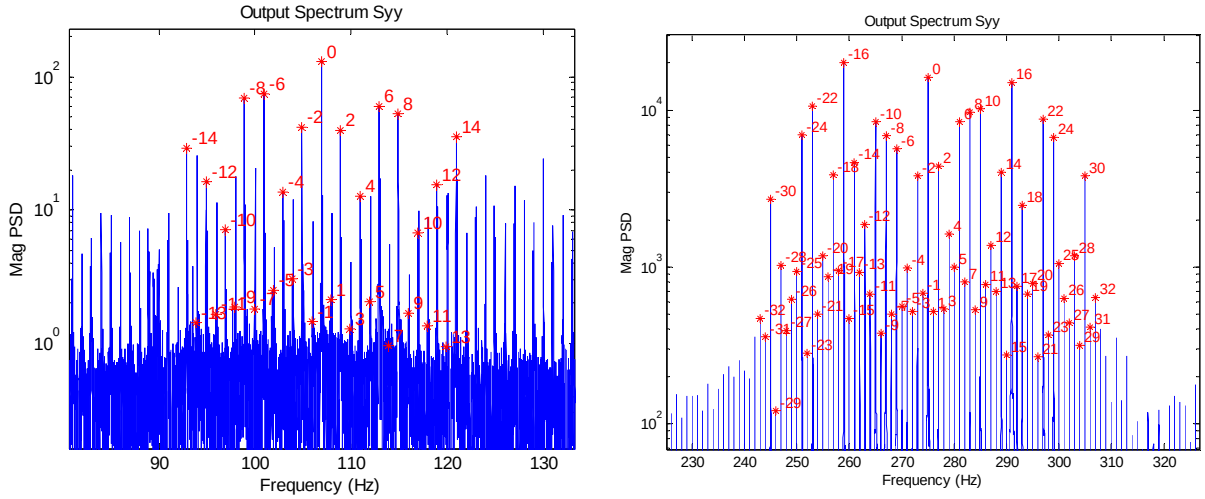

(a) (b)

Figure 5: Power Spectra of CSLDV signals for a) mode 1 and b) mode 4

Figure 6 compares the mode shapes obtained by CSLDV and 3D-DIC for the two linear steady state experiments. Figures 6a & 6b contain the mode shape at 106.9Hz and show good agreement between both measurement techniques and the FEM with a MAC of 0.9385 for CSLDV and 0.9274 for 3D-DIC. One difference between the measured and calculated mode shapes is a notable skew in the maximum deformation of the mode 1 shape, seen most clearly in Figure 6b. This skew is most likely due to the addition of the magnetic disk, as it is skewed toward the disk location, but could also be from the initial curvature previously discussed or a difference in clamping at the boundaries of the plate. Hence, there are most likely systematic differences between the FEA and measured mode shapes, so the fact that the MACs are not unity is not necessarily an indication of experimental error but information that will be useful when updating the FEM. On the other hand, since the linear measurement pertains to small

displacements one would expect the noise for 3D-DIC to be higher. The focus of this work was on modes of the plate that would be excited with the use of symmetric loading, so the next linear mode examined was mode 4. Since mode 4, is symmetric it can be excited with base excitation from the larger shaker. Figures 6c & 6d contain the mode shape at 277.70 Hz and again show good agreement between measurement and analysis with a MAC of 0.9408 for CSLDV and 0.9672 for 3D-DIC. There are again noticeable differences in the location of the maximum and minimum deformations of mode 4.

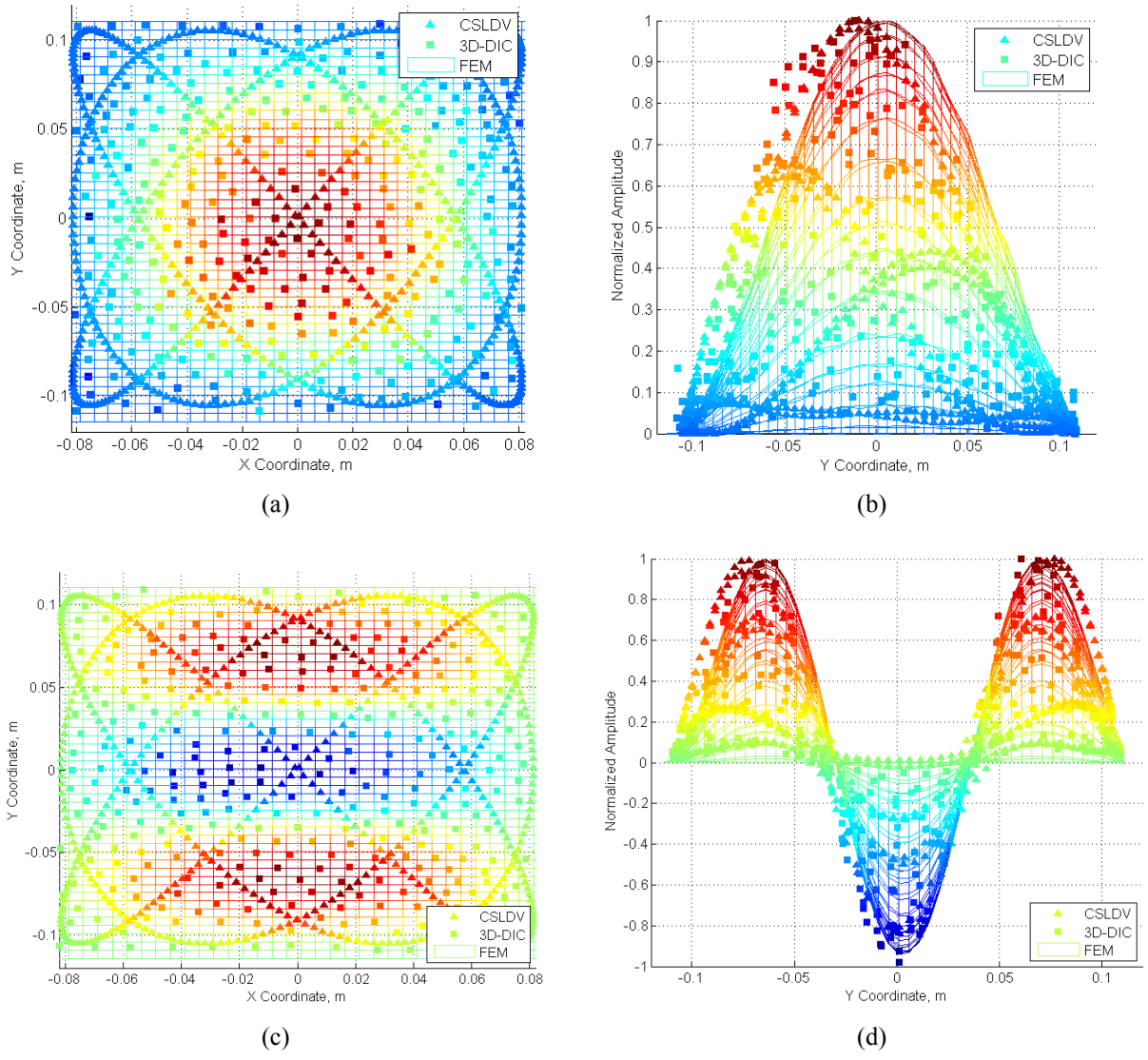

Figure 6: Mode Shape Comparison between CSLDV, 3D-DIC, and FEM: a) & b) Mode 1, c) & d) Mode 4

It is important to note that while the smooth nature of the CSLDV mode shapes seems to suggest that they are infallible, they are in fact an approximation of the true mode shapes obtained by expanding them in a Fourier series of the time-varying scan pattern. As mentioned previously, 28 clearly dominant harmonics (i.e. n=-14...14) were observed for the first mode. The neglected harmonics were an order of magnitude smaller than the dominant ones, so one would be inclined to have high confidence in that shape, but any feature that is too small to be represented in a 28-term Fourier series would not be captured. Another check of measurement confidence comes from the reconstruction of the Lissajous curve since the laser is scanning along a fixed pattern. When the measurements are noisy, the overlapping parts of the pattern tend to differ giving an indication of the error. Due to the complexity of the 2-D pattern, this is difficult to visualize here but when the 3D shapes are rotated it becomes apparent. An additional consideration for the accuracy of CSLDV comes as the mode shapes become more complicated, since more harmonics are needed accurately reconstruct the mode shape. This is evident in the mode 4, where even though more than twice as many side bands were used to reconstruct the shape, it appears to not have reconstructed the mode shape as accurately as 3D-DIC.

4.3 Nonlinear Deflection Shapes

As the magnitude of input excitation to a structure is increased such as this, geometric nonlinearity becomes more noticeable in the response. With the use of single-sine (or mono-harmonic) force appropriation, nonlinearity can be visible in the PSD of the response as harmonics of the mode frequency being excited [30]. This is illustrated in Figure 7a and 7b where the PSD of the 308 3D-DIC measurement locations and the CSLDV measurement for the response of the plate when excited in the first mode at 1.21g's of base acceleration is shown. The geometric nonlinearity of the plate for the first mode takes the form of spring hardening, where the natural frequency increases with increasing force amplitude. For instance, the linear frequency for mode 1 was 106.9Hz and this has increased to 160.8Hz (a 53.9Hz shift in natural frequency!) for this high amplitude excitation. In addition to the change in frequency, higher harmonics are seen at integer multiples of the forcing frequency and the deformation of the plate can be different at each of these harmonics. After transforming the measured deformations with 3D-DIC and CSLDV to the frequency domain the plate deformation at each of these harmonics of the forcing function can be examined.

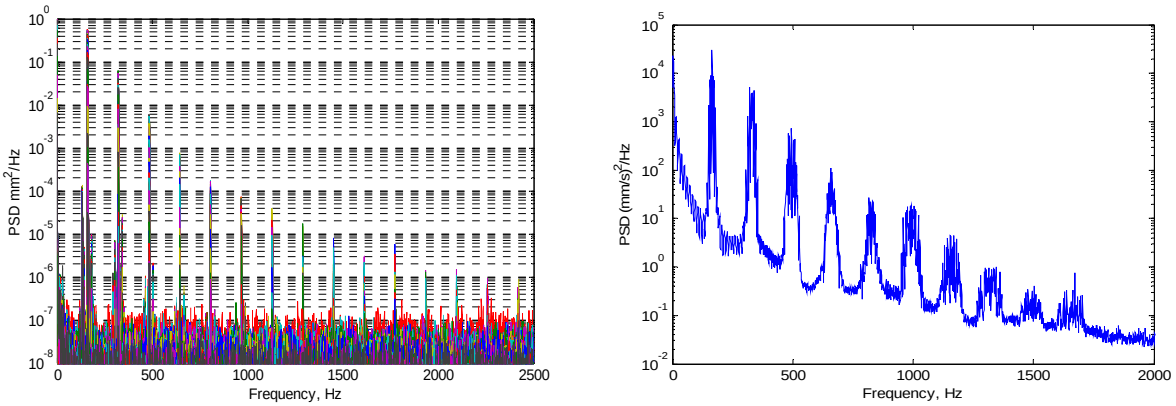

(a) (b)

Figure 7: Power Spectral Density of a) All 3D-DIC measurements, b) CSLDV vibrometer measurement

Here, the deformation shapes at each harmonic are reconstructed with CSLDV using 32 sideband harmonics, the same number that was used previously with the 4th linear mode shape. As is generally the case for a structure such as this [31], the primary harmonic of the measured nonlinear response, at 160.8Hz, resembles the first linear mode of the plate, as shown in Figure 8a and 8b. Both measurement systems capture this deformation well and are in good agreement with each other. The second harmonic of the nonlinear response, at 321.6Hz is shown in Figure 8c and 8d and was found to resemble the third linear mode of the plate. This deformation shape is unexpected since the base excitation that was used should theoretically not be able to directly excite an asymmetric mode such as this. Furthermore, the nonlinear normal modes [32] of a symmetric structure are typically all either purely symmetric or anti-symmetric [31, 33], so this measurement suggests that asymmetry is important to the nonlinear response and this information will be critical when modeling the structure. One should also note that asymmetric motions such as this are frequently observed in initially curved structures so the initial curvature of the plate should be modeled in the FEM. Again, both measurement systems are able to capture this slightly more complicated mode shape.

The third harmonic, at 482.4Hz, was found to resemble a rotated version of the 5th linear mode of the FEM as seen in Figure 9. This type of response is again unexpected as the characteristic shape is asymmetric in the y-coordinate. Again, both measurement systems capture the deformation shape well confirming the validity of this unexpected deformation shape. The fourth and the fifth harmonics showed similar results. The next harmonic examined is the sixth harmonic. Interestingly, the sixth harmonic's deformation shape, at 964.8Hz, resembles the 21st

mode of the FEM. Here, the deformation shape is far more complicated, calling into question the accuracy of a CSLDV shape based on only 39 Fourier terms. The shape does not agree with itself at several of the points where the lines of the Lissajous figure cross. Additional terms could easily be added when post processing the measurement, but the sideband harmonics greater than 39 at the sixth harmonic do not stand out from the noise sufficiently to warrant adding additional terms. The accuracy of the deformation shape with 3D-DIC is also called into question since the deformation at this frequency is small. An examination of Figure 9a shows small differences between adjacent measurement points that is more prominent at the peaks of deformation giving an indication of measurement error. However, this error is hard to fully define.

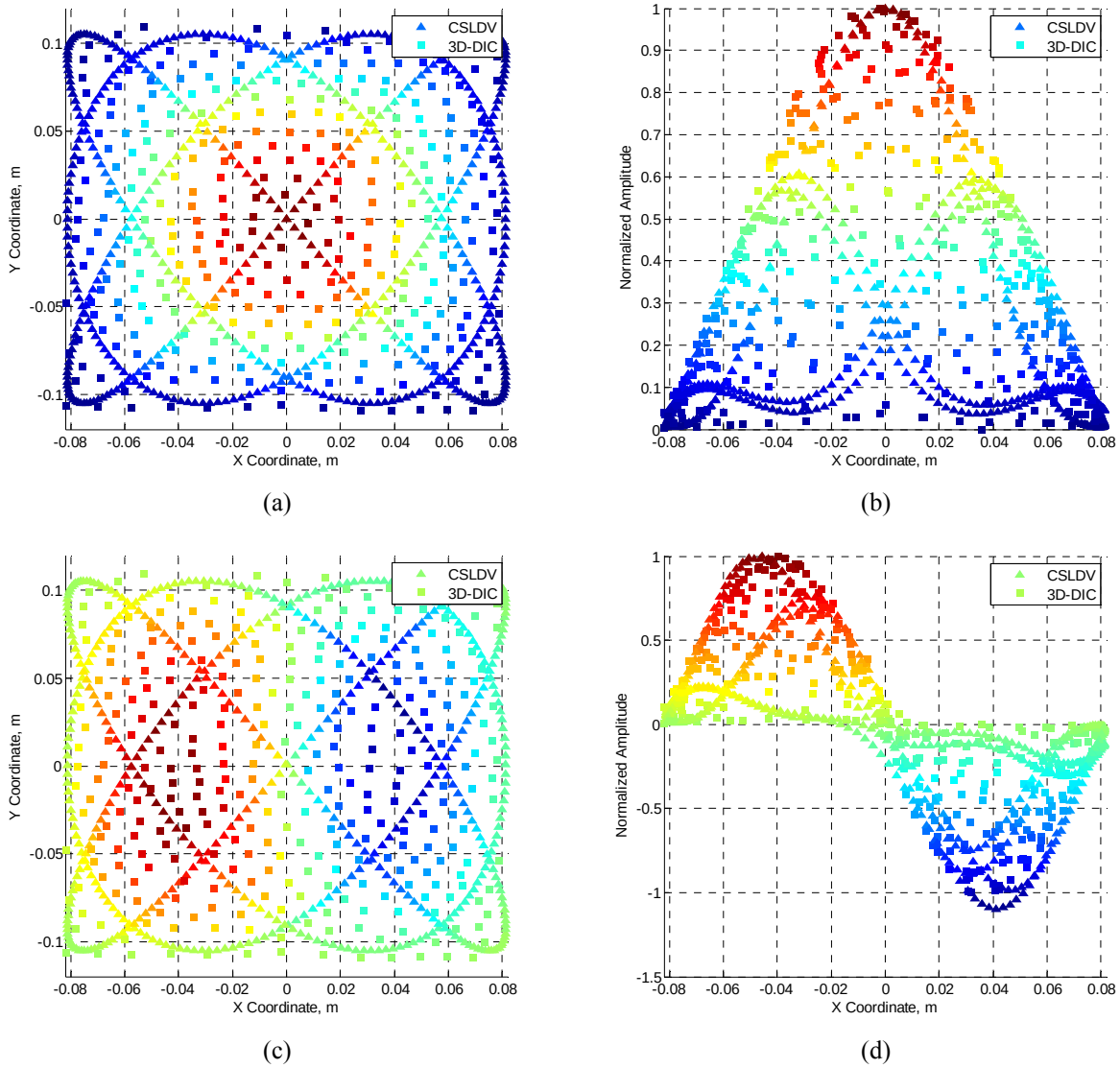

Figure 8: Deformation shape of CSLDV and 3D-DIC: a) & b) 1st harmonic, c) & d) 2nd harmonic

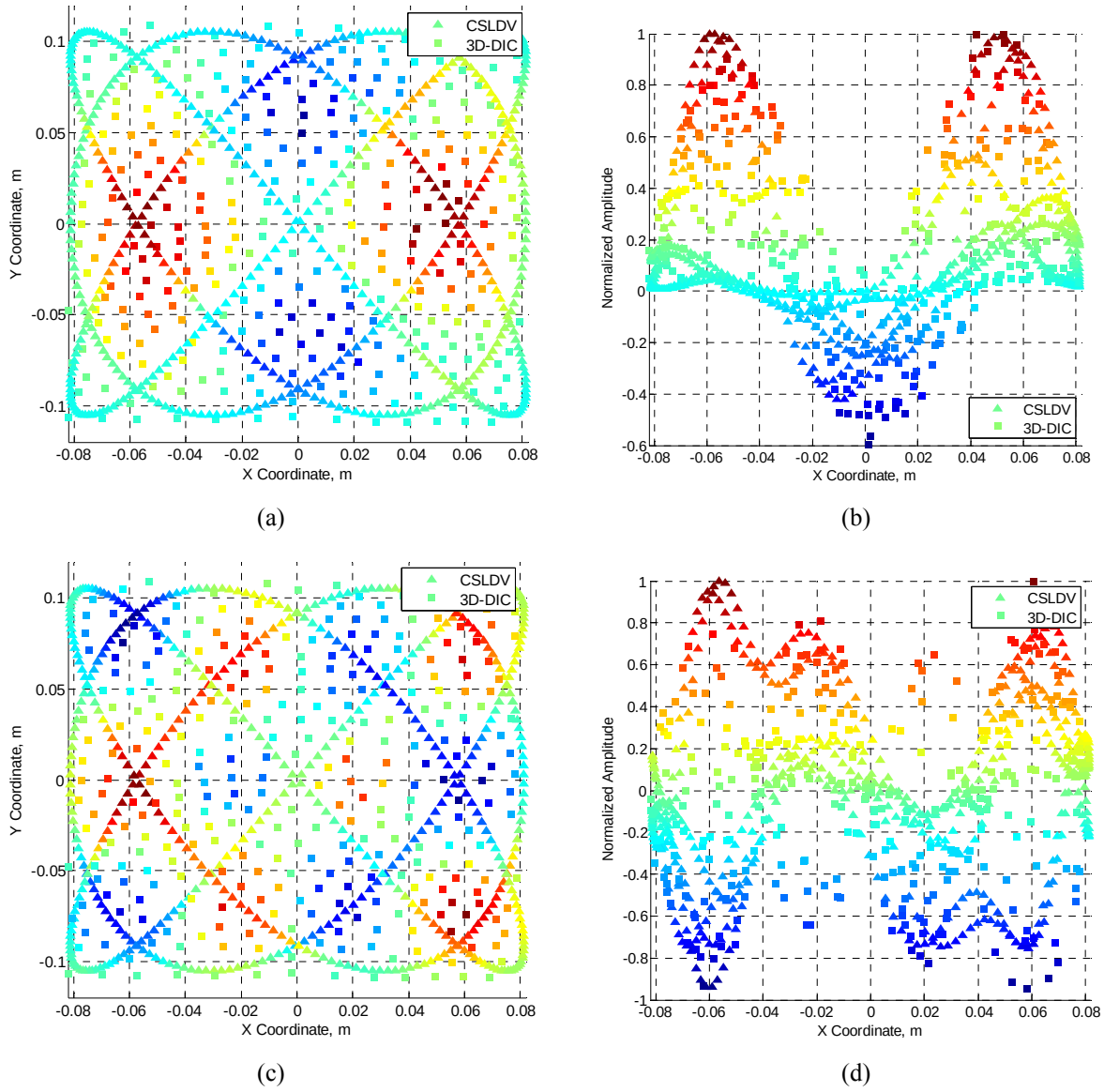

Figure 9: Deformation shape of CSLDV and 3D-DIC: a) & b) 3rd harmonic, c) & d) 6th harmonic

5 Conclusion

In this investigation, the dynamic response of a nominally flat clamped aluminum plate was examined. Between each test, the natural frequencies and damping ratios were identified using a single-input single-output modal hammer test in order to monitor the consistency of the plate, and they were found to exhibit minimal variation. The mode shapes and natural frequencies of the first and fourth modes of the plate were also identified using force

appropriation, with full-field dynamic deformations measured using CSLDV and high speed 3D-DIC. The results showed good agreement between the indentified linear frequencies and mode shapes and those calculated with the FEM. In addition to these linear measurements, nonlinear deformations of the first mode are also presented. Under nonlinear response conditions, full-field measurements allow the identification of nonlinear harmonics and the associated deformation shapes. This information is expected to be critical when seeking to update a nonlinear FE model of the structure, as the authors have begun to explore in [18], because there are often many ways in which the model may be updated to match the linear natural frequencies but nonlinear response predictions will not be accurate unless it also reproduces the correct nonlinear couplings between modes and the correct frequency-energy dependence for each mode.

Both techniques have shown the ability to provide dense measurements along surfaces, as long as each technique can "see" the surface throughout the deformation. To improve measurement accuracy, additional surface preparation is required, unless the material used for the test piece fulfills specific requirements (eg. a random pattern for 3D-DIC and a sufficiently reflective pattern for CSLDV). For DIC, this surface preparation is especially important when response levels are small, or in a structure's linear range. For CSLDV, surface preparation becomes more important when the vibration amplitude becomes small relative to speckle noise, and also as the laser standoff distance (or field of view) increases.

Acknowledgements

Support for this research was provided by the University of Wisconsin – Madison Graduate School with funding from the Wisconsin Alumni Research Foundation and through the Structural Sciences Center in the Air Force Research Laboratory's summer internship program.

References

[1] C. W. Schwingshackl, A. B. Stanbridge, C. Zang, and D. J. Ewins, "Full-Field Vibration Measurement of Cylindrical Structures using a Continuous Scanning LDV Technique," presented at the 25th International Modal Analysis Confernce (IMAC XXV), Orlando, Florida, 2007.

[2] A. B. Stanbridge and D. J. Ewins, "Modal Testing Using a Scanning Laser Doppler Vibrometer," *Mechanical Systems and Signal Processing,* vol. 13, pp. 255-270, 1999.

[3] A. B. Stanbridge, M. Martarelli, and D. J. Ewins, "Measuring area vibration mode shapes with a continuous-scan LDV," *Measurement,* vol. 35, pp. 181-9, 2004.

[4] M. Martarelli, "Exploiting the Laser Scanning Facility for Vibration Measurements," Ph.D. Ph.D., Imperial College of Science, Technology & Medicine, Imperial College, London, 2001.

[5] A. B. Stanbridge, A. Z. Khan, and D. J. Ewins, "Modal testing using impact excitation and a scanning LDV," *Shock and Vibration,* vol. 7, pp. 91-100, 2000.

[6] M. S. Allen, "Frequency-Domain Identification of Linear Time-Periodic Systems using LTI Techniques," *Journal of Computational and Nonlinear Dynamics* vol. 4, 24 Aug. 2009.
[7] S. Yang, M. W. Sracic, and M. S. Allen, "Two algorithms for mass normalizing mode shapes from impact excited continuous-scan laser Doppler vibrometry," *Journal of Vibration and Acoustics,* vol. 134, p. 021004, 2012.
[8] N. M. Wereley, "Analysis and Control of Linear Periodically Time Varying Systems," PhD, Department of Aeronautics and Astronautics, Massachusetts Institute of Technology, Cambridge, 1991.
[9] N. M. Wereley and S. R. Hall, "Linear time periodic systems: transfer functions, poles, transmission zeroes and directional properties," presented at the Proceedings of the 1991 American Control Conference, Boston, MA, USA, 1991.
[10] N. M. Wereley and S. R. Hall, "Frequency response of linear time periodic systems," Honolulu, HI, USA, 1990, pp. 3650-3655.
[11] S. Yang, "Modal Identification of Linear Time Periodic Systems with Applications to Continuous-Scan Laser Doppler Vibrometry," Ph.D Ph.D., Engineering Physics, University of Wisconsin-Madison, 2013.
[12] S. Yang and M. S. Allen, "Harmonic Transfer Function to Measure Translational and Rotational Velocities With Continuous-Scan Laser Doppler Vibrometry," *Journal of Vibration and Acoustics,* vol. 136, pp. 021025-021025, 2014.
[13] T. E. Schmidt, J. Tyson, K. Galanulis, D. M. Revilock, and M. E. Melis, "Full-field dynamic deformation and strain measurements using high-speed digital cameras," 2005, pp. 174-185.
[14] V. Tiwari, Sutton, M.A., Shultis, G., McNeill, S.R., Xu, S., Deng, X., Fourney, W.L., and Bretall, D., "Measuring full-field transient plate deformation using high speed imaging systems and 3D-DIC," in *Proceedings of the Society for Experimental Mechanics Annual Conference*, Albuquerque, 2009.
[15] C. Niezrecki, P. Avitabile, C. Warren, P. Pingle, and M. Helfrick, "A Review of Digital Image Correlation Applied to Structural Dynamics," *AIP Conference Proceedings,* vol. 1253, pp. 219-232, 2010.
[16] M. Helfrick, "3D Digital Image Correlation Methods for Full-Field Vibration Measurement," *Mechanical Systems and Signal Processing,* vol. 25, pp. 917-927, 2011.
[17] C. Warren, C. Niezrecki, P. Avitabile, and P. Pingle, "Comparison of FRF measurements and mode shapes determined using optically image based, laser, and accelerometer measurements," *Mechanical Systems and Signal Processing,* vol. 25, pp. 2191-2202, 2011.
[18] D. A. Ehrhardt, R. A. Harris, and M. S. Allen, "Numerical and Experimental Determination of Nonlinear Normal Modes of a Circular Perforated Plate," in *32nd International Modal Analysis Conference (IMAC XXXII)*, Orlando, Florida, 2014.
[19] M. S. Allen and B. Weekes, "Nonlinear Model Updating of a Flat Plate and a Stiffened Skin Panel from a Lynx Helicopter," presented at the Scitech 2015, 56th AIAA Structures, Structural Dynamics and Materials Confernece, Kissimmee, Florida, 2015.
[20] D. Ehrhardt, S. Yang, T. Beberniss, and M. Allen, "Mode Shape Comparison Using Continuous-Scan Laser Doppler Vibrometry and High Speed 3D Digital Image Correlation," in *Special Topics in Structural Dynamics, Volume 6*, G. Foss and C. Niezrecki, Eds., ed: Springer International Publishing, 2014, pp. 321-331.
[21] G. mbH, "Aramis," 6.3.0 ed. Braunschweig, Germany, 2011.
[22] G. mbH, "IVIEW Real Time Sensor," 6.3.0 ed. Braunschweig, Germany, 2011.
[23] N. M. Wereley and S. R. Hall, "Linear Time Periodic Systems: Transfer Function, Poles, Transmission Zeroes and Directional Properties," in *American Control Conference, 1991*, 1991, pp. 1179-1184.
[24] S. Yang and M. S. Allen, "Lifting approach to simplify output-only continuous-scan laser vibrometry," *Mechanical Systems and Signal Processing,* vol. 45, pp. 267-282, 2014.

[25] S. Yang and M. S. Allen, "Output-Only Modal Analysis Using Continuous-Scan Laser Doppler Vibrometry and Application to a 20kW Wind Turbine," *Mechanical Systems and Signal Processing,* vol. 31, August 2012 2011.
[26] M. A. Sutton, Orteu, J.J., and Schreier, H., *Image Correlation for Shape, Motion, and Deformation Measurements: Basic Concepts, Theory, and Applications*: Springer, 2009.
[27] D. A. Ehrhardt and T. J. Beberniss, "Experimental investigation of dynamic out of plane displacement error in 3D digital image correlation," in *54th AIAA/ASME/ASCE/AHS/ASC Structures, Structural Dynamics and Materials Conference, April 8, 2013 - April 11, 2013*, Boston, MA, United states, 2013.
[28] R. W. Gordon and J.J. Hollkamp, "Nonlinear Random Response of a Clamped Plate: A Well Characterized Experiment," presented at the 47th AIAA/ASME/ASCE/AHS/ASC Structures, Structural Dynamics, and Materials Conference, 2006.
[29] A. Gasparoni, M. S. Allen, S. Yang, M. W. Sracic, P. Castellini, and E. P. Tomasini, "Experimental Modal Analysis on a Rotating Fan Using Tracking-CSLDV," presented at the 9th International Conference on Vibration Measurements by Laser and Noncontact Techniques, Ancona, Italy, 2010.
[30] M. Peeters, G. Kerschen, and J. C. Golinval, "Modal testing of nonlinear vibrating structures based on nonlinear normal modes: Experimental demonstration," *Mechanical Systems and Signal Processing,* vol. 25, pp. 1227-1247, 2011.
[31] R. J. Kuether and M. S. Allen, "A Numerical Approach to Directly Compute Nonlinear Normal Modes of Geometrically Nonlinear Finite Element Models," *Mechanical Systems and Signal Processing,* vol. 46, pp. 1–15, 2014.
[32] G. Kerschen, M. Peeters, J. C. Golinval, and A. F. Vakakis, "Nonlinear normal modes. Part I. A useful framework for the structural dynamicist," *Mechanical Systems and Signal Processing,* vol. 23, pp. 170-94, 2009.
[33] R. W. Gordon and J. J. Hollkamp, "Reduced-order Models for Acoustic Response Prediction," Air Force Research Laboratory, AFRL-RB-WP-TR-2011-3040, Dayton, OH2011.